04,06

# Structure, microstructure and optical properties of $SrFe_{2/3}W_{1/3}O_3$ multiferroics thin films grown on MgO(001) substrate

© A.V. Pavlenko, A.V. Nazarenko, K.M. Zhidel', D.V. Stryukov

Southern Scientific Center, Russian Academy of Sciences,
Rostov-on-Don, Russia

E-mail: AntVPR@mail.ru

*Received July 30, 2025*
*Revised August 5, 2025*
*Accepted August 8, 2025*

The $SrFe_{2/3}W_{1/3}O_3$ multiferroic thin films were grown on a MgO(001) substrate using RF-cathode sputtering method in an oxygen atmosphere. It was found that the obtained $SrFe_{2/3}W_{1/3}O_3$ films are single-phase and single-crystal. According to the X-ray diffraction analysis they have a tetragonal unit cell with $a = b = 3.930$ Å and $c = 3.964$ Å parameters. It was shown that the $SrFe_{2/3}W_{1/3}O_3$ films exhibit transparency ($T = 62-75\,\%$) in the visible and near-IR wavelength ranges. The dispersion dependences of the refractive index $n(\lambda)$ and absorption coefficient $k(\lambda)$ of strontium ferrotungstate films were firstly determined in the wavelength range $\lambda = 350-1100$ nm using the spectral ellipsometry method.

**Keywords:** heterostructures, SWFO, ellipsometry, refraction index.

DOI: 10.61011/PSS.2025.08.62258.219-25

## 1. Introduction

Multiferroics, in which electric and magnetic orderings coexist at the temperatures above the room temperature, have been intensely studied in recent decades due to perspectives of their use in microelectronics and VHF technology [1,2]. Iron-containing perovskites $AFe_{2/3}W_{1/3}O_3$ ($A$ = Pb, Sr, Ba, Ca) are typical representatives of this class of materials. They were synthesized for the first time in the mid-1960s [2–4], but have started being studied only in the recent decades due to a growth of interest to the multiferroics with high temperatures of magnetic and ferroelectric phase transitions [5–8]. $SrFe_{2/3}W_{1/3}O_3$ (SFWO) is one of the most interesting representative of the said group of the materials, since it combines ferrimagnetic and ferroelectric properties when $T_m < 400$ K [9]. It is shown in the study [10] that when $T = 420-550$ K SWFO exhibits a smeared phase transition from a tetragonal (ferroelectric) into a cubic (paraelectric) phase. When jointly analyzing X-ray photoelectron and Mössbauer spectra of the SWFO ceramic at the room temperature, an oxygen shortage was detected and resulted in appearance of tungsten cations in an intermediate oxidation degree in their structures, whereas iron ions were only in a valence state $Fe^{3+}$ [9]. In turn, it is shown in the studies [5,11] that within the temperature interval 10–300 K SFWO has a tetragonal structure (a space group I4/m) and combines the ferrimagnetic and antiferroelectric properties at the temperatures below 373 K ($T_C = 473$ K). It is noted in the study [11] that an increase of the concentration of the iron ions results in appearance of the $Fe^{4+}$ cations in the SFWO structure and strong reduction of the magnetic transition temperature. All this indicates significant sensitivity of the structure and properties of this material to a thermodynamic manufacturing history, which is unfortunately inherent to many high-temperature multiferroics ($BiFeO_3$, $BiMnO_3$, etc.), whose structure includes cations with variable valence (Fe, Mn) [12,13]. Most likely, for this reason the SFWO compound in the form of the heteroepitaxial films is now unstudied. Taking into account that the strontium ferrotungstate multiferroic that is grown as thin films on the single-crystal substrates MgO, Si, $LaAlO_3$ and $Al_2O_3$, which are industrially used in VHF technology, optics and microelectronics, can be interesting both fundamentally and applicably, development of the production technology and analysis of the properties of these films are undoubtedly relevant for physical materials science.

The present study presents results of study of the crystal structure and the optical properties of the SFWO|MgO(001) films, which were manufactured for the first time using a single-stage method of high-frequency cathode dissipation.

## 2. Methods of sample preparation and study

The SFWO films were grown in an installation of the „Plasma 50 SE“ type, in which a target was a dedicated ceramic disc of the stoichiometric SFWO composition of the diameter of 50 mm, the thickness of 5 mm and relative density $\sim 92\,\%$. The substrate was a single-crystal (001)-cut MgO plate prepared for heteroepitaxial deposition (OST Photonics, double-sided polishing, of the thickness of 500 $\mu$m). The substrate temperature at the deposition start was $\sim 400\,^\circ$C and the distance between the target and a furnace was 12 mm. The film was totally synthesized in

the atmosphere of pure oxygen at the chamber pressure $\sim 0.5$ Torr and the film was directly deposited for 60 min.

X-ray diffraction studies of the samples at the room temperature were carried out in a multifunctional X-ray complex „RICOR“ (the Bragg-Brentano geometry, goniometer with an increment of up to 0.001°) (Crystal Logic Inc.), an X-ray tube BSV21-Cu (JSC „Svetlana-Rentgen“), a scintillation detector (LLC ITC „Radikon“).

The microstructure and the elemental composition of portions of the film surface were studied using a scanning electron microscope (SEM) Carl Zeiss EVO 40 (Germany) with an additional energy-dispersive analysis add-on by „Inca Oxford Instruments“. Electron emission was produced by means of a standard tungsten cathode (a V-shaped tungsten thread of the diameter $\sim 100\,\mu$m). An additional conducting layer was not deposited on the surface of the studied film. The spectra were accumulated in a mode of increased probe current $I_{\text{probe}} = 500$ pA at an accelerating voltage EHT = 20 kV. A working distance was WD = 8.5 mm, while a spectrum accumulation time was $\tau = 50$ s.

The film transmission spectra were studied in a spectrophotometer SF-56 (OKB „Spektr“, Russian) with in the wavelength range from 200 to 1100 nm. Optical constants and the thickness of the thin-film structures were determined by means of spectral studies using an ellipsometry method that was based on investigating a state of polarization of reflected light after its interaction with a surface of two-media interfaces The measurements were performed by means of spectral ellipsometer „ELLIPS-1991“ (LLC NPK „TsNT“, Russia) designed to operate in a static diagram within the wavelength range $\lambda = 350-1000$ nm. The spectral resolution was 2.5 nm. The measurement time for one spectrum did not exceed 20 s. The spectral dependence of the ellipsometric parameters $\Psi$ and $\Delta$ was taken with an increment of 2 nm at a fixed light incidence angle of 65°. The measurements were carried out using a four-zone method [14]. It included determining the ellipsometric angles $\Psi$ and $\Delta$ that are included in the main ellipsometry equation:

$$\rho = r_p/r_s = \text{tg} \cdot \exp(i\Delta), \qquad (1)$$

where $\text{tg}\,\Psi = |r_p|/|r_s|$ is a ratio of complex reflection coefficients $r_p$ and $r_s$ and $\Delta = \delta r_p - \delta r_s$ is a relative phase change tested in reflection between $p$- and $s$-components. The optical parameters of lenses were calculated using built-in „Spectroscan“ software.

## 3. Experimental results and discussion

The X-ray diffraction method was used to study the crystal structure of the SFWO thin film grown on the MgO(001) substrate. Shooting in a $\theta - 2\theta$ standard geometry (Figure 1) showed presence of reflections from a family of planes (00l), thereby indicating coaxiality of axes [001] of the film and substrate.

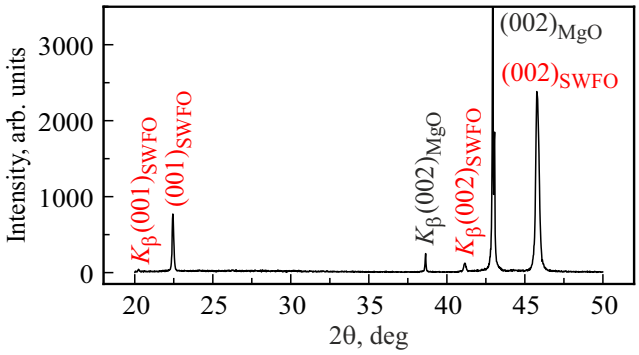



**Figure 1.** $\theta - 2\theta$ X-ray diffraction pattern of the SFWO|MgO(001) film.

In order to determine orientation of the lattice cell of the film relative to the substrate, we have obtained $\varphi$-scans of the reflections of the film (103) and of the substrate (113) (Figure 2, *a*).

The obtained X-ray diffraction patterns have four bright maximums that belong to scattering by the SFWO film, thereby proving its epitaxial growth. Angular positions of the film reflections relative to the substrate reflections indicate parallelism of all the crystallographic axes of the film and the substrate. The observed displacement of 45° is related to selection of the reflections for the film (103) and for the substrate (113). It should be noted that no single trace of impurity phases is detected on all the obtained X-ray diffraction patterns at the various shooting geometries, thereby confirming a high quality of the produced films in addition to small widths of all the reflections. The film is also characterized by low values of disorientation of the crystallographic axes: vertical disorientation is below 1° (Figure 2, *b*), whereas azimuthal disorientation is below 3.1° (Figure 2, *a*). In order to determine the parameters of the lattice cell, a family of the reflections (00$l$) and the reflection (103) were precisely shot. Due to shooting four orders of the reflection (00$l$), we managed to determine the parameter $c = 3.964$ Å with accuracy of $\pm 0.001$ Å. The reflection (103) was shot with rotation along $\varphi$ by 90°, where it is possible to note that the rotation does not result in displacement of the angular position of the reflection. Thus, it is most likely that the SFWO film has the tetragonal lattice cell with the parameter $a = b = 3.93$ Å with accuracy of $\pm 0.01$ Å. Deformation of the lattice cell of the film as compared to the bulk material ($a = 3.943$ Å, $c = 3.955$ Å [10]) is $-0.33\,\%$ in an interface plane and $0.23\,\%$ along the normal to the substrate surface, thereby indicating an increase of a tetragonality degree of the lattice cell in the SFWO films.

The microstructure was analyzed to show that the surface of the produced film is homogeneous. Pores, caverns and impurity inclusions are not observed. Without the additional conducting layer, the surface originated charging effects that were manifested as heterogeneous contrast and dark spots — areas, whence the electrons migrated. The

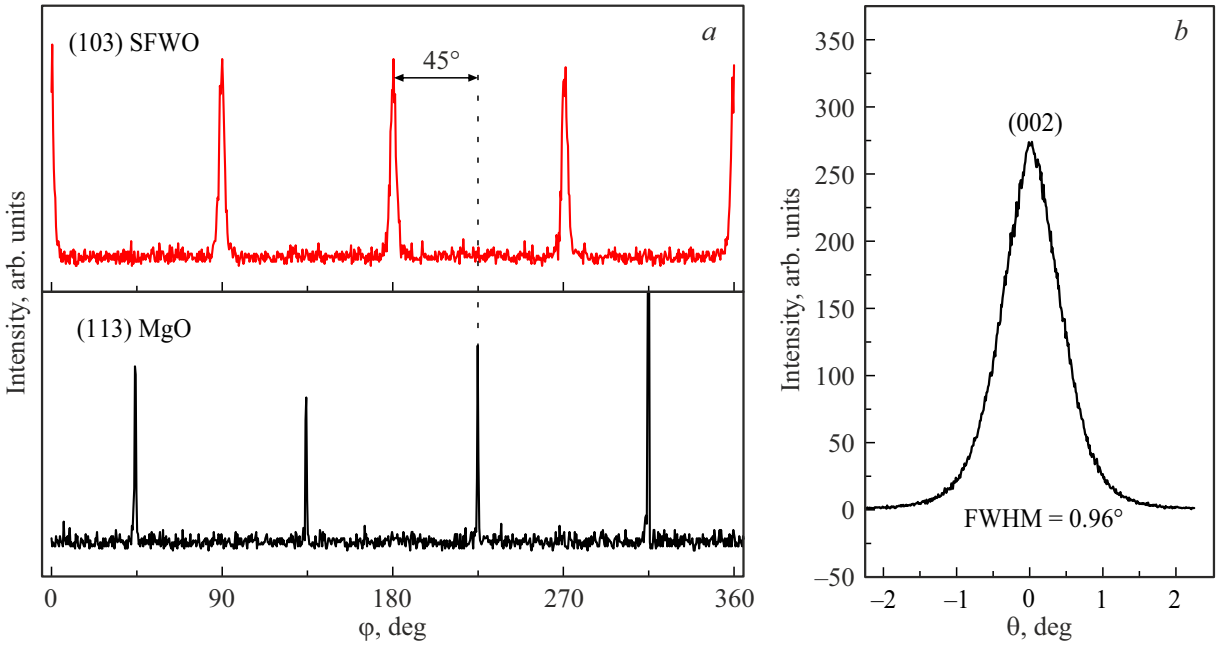



**Figure 2.** *a*) $\varphi$-scannings of the reflections of the film (103) and of the substrate (113) for the SFWO|MgO(001) film and *b*) the rocking curve for the reflection (002) of the SFWO film.

elemental composition was studied from a surface of the size $\sim 100 \times 80\,\mu$m. The results showed presence of the elements included in the composition both of the substrate and the studied heterostructure. It can be noted that all the elements of the dissipated target are included in the film composition. However, since the most intense signals from sets of L-lines of strontium (Sr) and M-lines of tungsten (W) fall within the same energy range $E_{\text{Sr-L}} = E_{\text{W-M}} = 1.75-1.95$ keV, the reflection of Sr and W are merged. If presence of the W element is confirmed by a quite intense peak from the set of its L-lines ($E_{\text{W-L}} = 8.3-8.5$ keV), then the Sr element in the spectra accumulated for the time $\tau$ was not reliably confirmed. In order to verify presence of these elements, a more detailed spectrum (Figure 3) was obtained, which was accumulated not for the $\tau$, but by the number of recorded electrons ($N \approx 2 \cdot 10^5$).

Thus, we managed to increase the intensity of the entire spectrum and resolve a part of the lines not only of the said sets (Figure 3, the insert), but of other electron shells of Sr and W.Thus, now one can well see presence of additional peaks of W within the energy range $E_{\text{W-L}} = 9.5-10.2$ keV and the Sr reflection of the set of the K-lines appeared as well when $E_{\text{Sr-K}} = 14.0-14.4$ keV. Relative weight and atom ratios of the elements are given in the table.

Reliability of the quantity results was improved by averaging the data obtained based on the energy-dispersive spectra that were accumulated in the various points of the surface. The quantity analysis results show good agreement of the compositions of the film and the dissipated target [15].

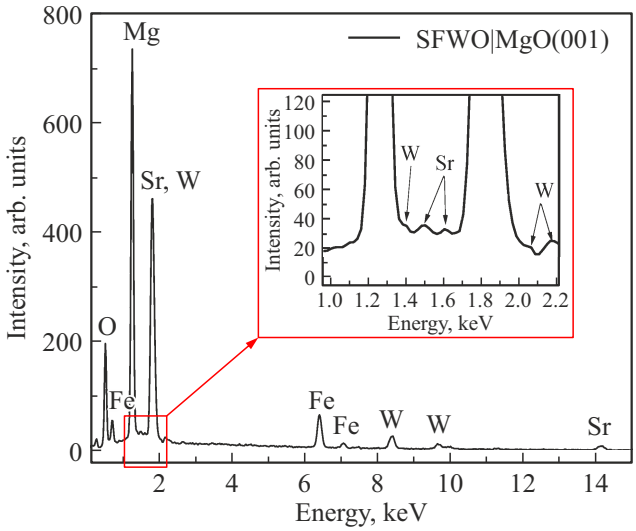



**Figure 3.** Typical energy-dispersive spectrum of the portion of the surface of the SWFO|MgO(001) film.

The chemical elements were mapped over the entire studied surface to show that all the ions were distributed quite homogeneously. For clarity, Figure 4 shows distributions of the main elements included in the film.

It is clear that for the said atoms there are not separate clusters that could indicate presence of areas of their increased concentration. It also confirms absence of the impurity inclusions and the good quality of the produced heterostructure. The difference occupancy of Sr, W and Fe seems to be related to the fact that the presented elements

Results of quantity analysis of the elemental composition of the portion of the surface of the SWFO|MgO(001) film

| Element* | Wt% | $\sigma_{wt}$, % | At. % |
|---|---|---|---|
| O (K-line) | 25.41 | 0.51 | 50.70 |
| Mg (K-line) | 24.50 | 0.36 | 32.17 |
| Fe (K-line) | 8.34 | 0.23 | 4.71 |
| Sr (L-line) | 26.76 | 0.59 | 9.31 |
| W (M-line) | 15.00 | 0.75 | 2.62 |

Note. * The parentheses include the basic line used for calculation.

are calculated by electrons from the different electron shells (see Table).

The transmission spectrum of the SFWO|MgO heterostructure is shown in Figure 5. It is clear that the transmission coefficient ($T$) of the SFWO films within the spectral range from 570 to 1100 nm varies within the range from 62 to 75 % on the MgO substrate. The transmission spectrum indicates that the SFWO thin films are characterized by a flat surface and demonstrate a good degree of homogeneity. In the optical absorption edge region, light transmission of the films monotonically decreases to zero. The dependences of the ellipsometric angles $\Psi$ and $\Delta$ on the wavelength for the studied sample of the SFWO film on the MgO substrate are shown in Figure 6. In order to calculate the dependences of the optical constants based on the experimental dependences $\Psi(\lambda)$ and $\Delta(\lambda)$, we used a solution of the ellipsometry inverse problem according to the equation (1) for the optical model „the MgO substrate | the SFWO film | the surface layer". The surface layer describes the presence of roughness.

The thickness of the surface layer was selected so as to minimize a discrepancy between the experimental and calculated values. Roughness was taken into account when calculating the parameters by adding the surface layer to the structure, whose optical constants were determined by the Bruggeman model. The surface-layer model is a surface layer with the same optical constants that the main film has, but with an introduced fraction of cavities (air). The search results are shown in Figure 6 (the solid lines). It is clear that there is good convergence between the calculation and the experiment. The thickness of the SFWO main layer that was determined within the framework of the used optical model was 259 nm. The obtained results suggest that boundary layers at the MgO-SFWO interfaces are lacking and the thickness of the surface layer on a free surface of the structure does not exceed 3.2 nm includes 39 % of cavities. It should be noted that the obtained parameters of the surface layer are confirmed and found in accordance with additional studies of the surface of the SWFO film by atomic force microscopy (a value of RMS roughness of the film on the typical surface area of 25 $\mu m^2$ was 2.64 nm).

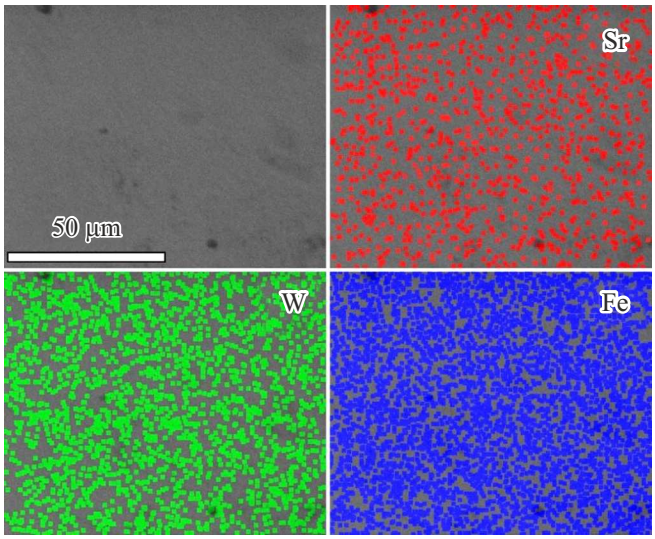



**Figure 4.** Results of mapping of the elements Sr, W and Fe over the studied part of the surface of the SWFO|MgO(001) film.

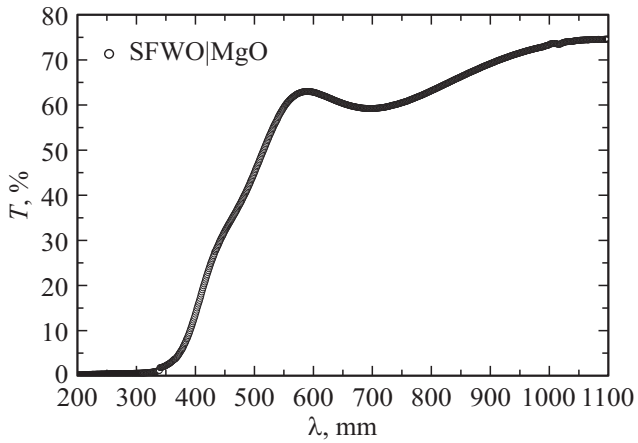



**Figure 5.** Transmission spectrum of the SFWO|MgO films and the MgO substrate.

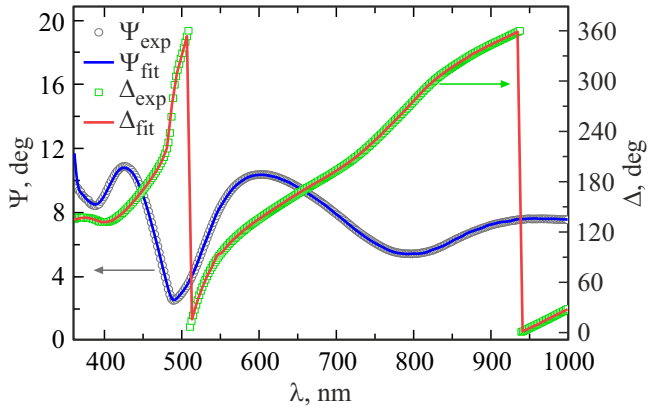



**Figure 6.** Dependences $\Psi(\lambda)$ and $\Delta(\lambda)$ of the SFWO|MgO films.

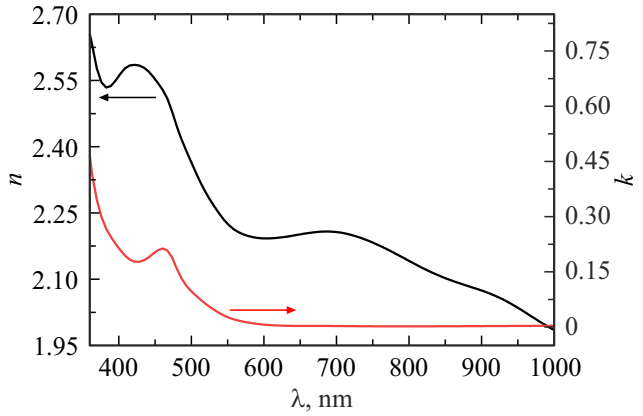



**Figure 7.** Dependences $n(\lambda)$ and $k(\lambda)$ of the SFWO film.

Figure 7 shows dispersion dependences of the refractive index $n(\lambda)$ and the absorption index $k(\lambda)$ of the SFWO film.

Unfortunately, it was not possible within the framework of the present study to find in the literature data about the value of the refractive index for the bulk strontium ferrotungstate materials of the $SrFe_{2/3}W_{1/3}O_3$ composition. In this regard, for comparison purposes we have used the refractive index of lamellar perovskite of the $Sr_2FeWO_6$ composition in the visible spectral range, which is ab initio calculated by the density functional theory and represented in the study [16]. A spread of values of the real part of the refractive index $Sr_2$ of $FeWO_6$ is within the range from 1.7 to 2.8 in a dependence on an applied pressure within the interval from 2 to 10 GPa [16]. Despite a lack of literature data for the studied material, the performed analysis makes it possible to justifiedly compare based on the available theoretical calculations and the experimental results for the related compound. The obtained values ($n(\lambda) = 1.98-2.68$ within the range $\lambda = 350-1000$ nm) are close to those presented in the study [16] for $Sr_2FeWO_6$.

## 4. Findings and conclusion

It was studied to show that using the high-frequency cathode dissipation in the oxygen atmosphere on the MgO(001) substrate made it possible to produce the SFWO single-crystal films that exhibited full parallel orientation of the crystallographic axes of the films relative to the substrate axes and the increase of the tetragonality degree $(c/a)$ of the lattice cell from 1.003 to 1.0086. Based on the data of X-ray diffraction analysis, SEM (energy-dispersive analysis) and spectroscopic ellipsometry, no features of presence of the impurity phases, breach of the chemical composition or other surface defects were detected in the SFWO|MgO(001) heterostructure.

The analysis by means of the mutually complementary methods of spectrophotometry and spectroscopic ellipsometry of the optical properties of the SFWO|MgO(001) film has shown that they demonstrate high transparency in the visible and near-IR wavelength ranges. In turn, the refractive index within the wavelength range $\lambda = 350-1000$ nm is $n(\lambda) = 1.98-2.68$.

It is important to note that even at the thickness $\sim 259$ nm the SWFO single-crystal films that are produced by us for the first time have significant deformation of the lattice cell, which makes it possible to expect a significant change of the dielectric and ferroelectric properties as compared to the ceramic, which will be done by us in further studies. It makes sense to use the obtained results in producing and studying the properties of the heterostructures based on the SFWO films.

### Acknowledgments

The authors would like to thank CUC of Joint Scientific and Technological Equipment Center of the Southern Scientific Center of the Russian Academy of Sciences (Research, Development, Testing) (https://ckp-rf.ru/catalog/ckp/501994/) for provided equipment for the studies.

### Funding

The study was supported by grant No. 25-22-00476 from the Russian Science Foundation, https://rscf.ru/project/25-22-00476/.

### Conflict of interest

The authors declare no conflict of interest.

## References

[1] T. Kimura, T. Goto, H. Shintani, K. Ishizaka, T. Arima, Y. Tokura. Nature **426**, *6962*, 55 (2003).
[2] A.P. Pyatakov, A.K. Zvezdin. Phys. — Uspekhi **55**, *6*, 557 (2012).
[3] E.G. Fesenko. *Semeistvo perovskita i segnetoelektrichestvo.* Atomizdat, M. (1972). 248 s. (in Russian).
[4] G. Blasse. J. Inorg. Nucl. Chem. **27**, *5*, 993 (1965).
[5] S.A. Ivanov, S.-G. Eriksson, R. Tellgren, H. Rundlof. Mater. Res. Bull. **36**, *15*, 2585 (2001).
[6] S.A. Ivanov, S.G. Eriksson J. Erikssen, R. Tellgren, H. Rundlof. Mater. Res. Bull. **39**, *4–5*, 615 (2004).
[7] S.A. Ivanov, S.-G. Eriksson, R. Tellgren, H. Rundlof, P. Nordblad, J. Eriksen. J. Solid State Chem. **179**, *8*, 2645 (2006).
[8] S. Vasala, M. Karppinen. Progr. Solid State Chem. **43**, *1–2*, 1 (2015).
[9] A.V. Pavlenko, S.P. Kubrin, A.T. Kozakov, L.A. Shilkina, L.A. Reznichenko, A.V. Nikolskii, V.V. Stashenko, Y.V. Rusalev, K.S. Petrosyan. J. Alloys. Compd. **740**, 1037 (2018).
[10] A.V. Pavlenko, A.V. Turik, L.A. Shilkina, S.P. Kubrin, Yu.V. Rusalev, L.A. Reznichenko, I.N. Andryushina. Phys. Solid State **60**, *3*, 515 (2018)
[11] M. del C. Viola, M.S. Augsburger, R.M. Pinacca, J.C. Pedregosa, R.E. Carbonio, R.C. Mercader. J. Solid State Chem. **175**, *2*, 252 (2003).

[12] J. Silva, A. Reyes, H. Esparza, H. Camacho, L. Fuentes. Integrated Ferroelectrics **126**, *1*, 47 (2011).
[13] D.V. Karpinsky, M.V. Silibin, D.V. Zhaludkevich, S.I. Latushka, V.V. Sikolenko, D.M. Többens, D. Sheptyakov, V.A. Khomchenko, A.A. Belik. Mater. **14**, *19*, 5805 (2021).
[14] V.A. Shvets, E.V. Spesivtsev, S.V. Rykhlitskii. Optics. Spectroscopy **97**, *3*, 483 (2004).
[15] A.V. Nazarenko, G.V. Valov, A.V. Pavlenko. Nauka Yuga Rossii, **18**, *1*, 12 (2022). (in Russian).
[16] P. Mondal, N.A. Shahed, S. Khanom, M.K. Hossain, F. Ahmed. Mater. Sci. Eng.: B **298**, *9*, 116875 (2023).

*Translated by M.Shevelev*